ELSEVIER

Journal of Alloys and Compounds 275–277 (1998) 209–213

Journal of ALLOYS AND COMPOUNDS

Submillimeter EPR spectroscopy of lanthanide compounds: Pair centers of Ho^{3+} in $CsCdBr_3$

B.Z. Malkin[a,*], A.I. Iskhakova[a], V.F. Tarasov[b], G.S. Shakurov[b], J. Heber[c], M. Altwein[c]

[a]*Physics Department, Kazan State University, Kazan 420008, Russian Federation*
[b]*Kazan Physical-Technical Institute, Kazan 420029, Russian Federation*
[c]*Technical University of Darmstadt, Darmstadt D-64289, Germany*

Abstract

High-frequency EPR spectra corresponding to magnetic dipole transitions between the doublet–singlet–doublet group of the lowest crystal field levels of the trigonal single ion and the symmetric dimer centers in $CsCdBr_3$ have been studied. For the dimer center, the absorption spectra in the manifold of the lowest 1024 electron-nuclear states are simulated by successive diagonalization of the electron-nuclear Hamiltonian which includes the crystal field, the electronic Zeeman energies, the magnetic and quadrupole hyperfine interactions, and the dipole–dipole interactions between the paramagnetic ions. The crystal field parameters of Ho^{3+} ions in the symmetric dimer are determined. © 1998 Elsevier Science S.A.

Keywords: Crystal field; Holmium; Hyperfine structure; Paramagnetic resonance

1. Introduction

The spectral parameters of Kramers and non-Kramers ions can be measured by submillimeter electron paramagnetic resonance (EPR) which opens the possibility of observing the hyperfine structure of transitions between crystal field levels of the ground state of a lanthanide ion [1–3]. The specific shape of the hyperfine structure and the dependence of the resonance frequencies on the magnitude and the direction of the applied magnetic field complete substantially the information obtained by site-selective optical spectroscopy. They allow us to identify unambiguously the energy levels of different optical centers and to choose the proper crystal field Hamiltonian.

In this communication, the results of experimental and theoretical investigations of the EPR spectra of dopant Ho^{3+} ions in the hexagonal double bromide $CsCdBr_3$ are summarized. They were recorded at liquid helium temperatures with backward-wave oscillators in the frequency range 160–360 GHz and for magnetic fields up to 1 T (some preliminary results have been reported in Ref. [4]). The specific feature of these crystals doped with trivalent lanthanide ions is the presence of strong positional correlations among the impurity ions. They preferentially form symmetric dimer centers of the type Ln^{3+}–Cd^{2+} vacancy–Ln^{3+} substituting for three adjacent Cd^{2+} ions in the linear chain of confacial ($CdBr_6$) octahedra [5]. These pair centers have D_{3d} symmetry. The distance between the Ln^{3+} ions attracted by the Cd^{2+} vacancy diminishes from the lattice constant $c=6.722$ Å down to 5.94 Å [5,6]. The point symmetry of the impurity site itself is C_{3v}.

In $CsCdBr_3$, the $^5I_8$ ground state of the Ho^{3+} ($4f^{10}$) ion is split predominantly by the cubic part of the crystal field (which is similar to the crystal field in elpasolite hosts [7]), resulting in a ground doublet E and the nearest triplet T_1. For centers of trigonal symmetry, the triplet state is split further into a singlet Γ_2 and a doublet Γ_3 (the energy levels are labeled by their C_{3v} group irreducible representations). The optical spectra of $CsCdBr_3$:Ho^{3+} were studied in Ref. [8] by selective laser excitation. The extensive set of energy levels has been assigned to the principal dimer center (a part of this set is given in Table 1) including the first excited singlet Γ_2 at 5.5 cm^{-1} and the doublet at 9 cm^{-1}. Due to their low excitation energies and the relatively high concentration of the pair centers, $CsCdBr_3$:Ho^{3+} crystals are suitable for studying the peculiarities of the high-frequency EPR spectra of paramagnetic dimers.

In addition to the crystal field Hamiltonian

*Corresponding author. Tel.: +7 8432 362537; fax: +7 8432 380994; e-mail: boris.malkin@ksu.ru

0925-8388/98/$19.00 © 1998 Elsevier Science S.A. All rights reserved.
PII: S0925-8388(98)00305-3

Table 1
Energy levels of Ho^{3+} ions in the symmetric pair center in $CsCdBr_3$ (values in cm^{-1}). The point of reference for each multiplet is the lowest sublevel (the measured energy is given in parentheses). Experimental data not confirmed by calculations are marked by an asterisk

$^5I_8$	Γ_3	Γ_2	Γ_3	Γ_1	Γ_3	Γ_2 (Γ_3^*)	Γ_3	Γ_1	Γ_1	Γ_3 (Γ_2^*)	Γ_3	
	0	5.5	9.0	26.0	155.0	162.0	178.0	188.5	190.5	217.0	237.0	
	0	5.4	9.0	27.7	155.0	161.3	178.8	189.1	194.4	214.7	226.7	
$^5I_7$	Γ_3	Γ_2	Γ_3	Γ_1	Γ_3^*	Γ_2	Γ_3	Γ_1 (Γ_2^*)	Γ_3	Γ_2	Γ_3	Γ_1^*
	0 (5092.8)			2.2	73.2*	81.2	94.2	89.7	102.7	122.2	143.7	192.7*
	0	0.11	2.85	4.5		80.3	91.2	100.2	102.0	120.1	133.0	
$^5I_6$	Γ_3	Γ_1	Γ_3	Γ_2	Γ_1^*	Γ_3	Γ_1	Γ_3	Γ_2	Γ_1	Γ_3^*	Γ_1^*
		0 (8595.5)	10.5	29.0	45.5*	75.0		86.0	112.5		140.0*	173.0*
	−2.4	0	9.5	37.8		76.9	81.7	91.4	107.5	113.4		
$^5I_5$	Γ_2	Γ_3	Γ_3	Γ_1	Γ_3	Γ_2	Γ_3					
	0 (11164)	7.5	27.5		57.5	63.5	84.5					
	0	6.0	36.1	36.6	75.4	82.9	96.0					
$^5I_4$	Γ_3	Γ_3	Γ_1	Γ_2	Γ_1	Γ_3						
	0 (13215.5)			5.5	122.5	154.0						
	0	2.9	6.0	6.6	150.1	170.2						
$^5F_5$	Γ_3	Γ_2	Γ_3	Γ_1	Γ_3	Γ_3	Γ_2					
	0 (15307.5)	7	34	104.0*	134.7	163.5	175.5					
	0	3.6	49.1	54.0	155.7	178.8	187.1					

$$H_{\mathrm{cf}} = B_2^0 O_2^0 + B_4^0 O_4^0 + B_6^0 O_6^0 + B_4^3 O_4^3 + B_6^3 O_6^3 + B_6^6 O_6^6 \tag{1}$$

where O_p^k are the Stevens operators, each Ho^{3+} site is characterized by the nuclear hyperfine interaction of ^{165}Ho (nuclear spin $I=7/2$, 100% abundant). Thus, in the presence of an applied magnetic field $\boldsymbol{B}$ and neglecting the nuclear Zeeman energy and the extraionic quadrupole interaction, the Hamiltonian for a single Ho^{3+} ion (i) may be written in the following form:

$$\begin{aligned} H_i = {} & H_{\mathrm{cf}i} + g_J \mu_{\mathrm{B}} \boldsymbol{B} \boldsymbol{J}_i + A \boldsymbol{J}_i \boldsymbol{I}_i \\ & + \frac{3C}{4I(2I-1)J(2J-1)} \Big[\frac{1}{3}(3J_{zi}^2 - J(J+1))(3I_{zi}^2 \\ & - I(I+1)) + \frac{1}{2}(J_{-i}^2 I_{+i}^2 + J_{+i}^2 I_{-i}^2) + \frac{1}{2}(J_{zi} J_{-i} \\ & + J_{-i} J_{zi})(I_{zi} I_{+i} + I_{+i} I_{zi}) + \frac{1}{2}(J_{zi} J_{+i} + J_{+i} J_{zi})(I_{zi} I_{-i} \\ & + I_{-i} I_{zi}) \Big] \end{aligned} \tag{2}$$

where μ_{B} is the Bohr magneton, g_J is the Lande factor, $\boldsymbol{J}$ is the total electronic angular momentum, A is the constant of the magnetic hyperfine interaction, and C is the constant of the quadrupole interaction arising from the intra-ionic 4f shell. For the free ion $A=0.812$ GHz and $C=1.764$ GHz [9]. Due to the specific shape of the hyperfine structure in the EPR spectrum of a dimer center, containing two equivalent Ho^{3+} ions coupled together by a magnetic dipole–dipole interaction, we could unambiguously select the corresponding resonance lines. No deviations from the exact C_{3v} symmetry of the Ho^{3+} sites discussed in Ref. [8] were found. The energy level scheme for the symmetric dimer center obtained in Ref. [8] is well described by crystal field parameters for C_{3v} symmetry fitted to the measured magnetic field dependence of the hyperfine components of the EPR signals.

2. Experimental data

Single crystals of $CsCdBr_3$:Ho^{3+} were grown by the Bridgeman method. The procedure has been described previously [10]. The concentration of Ho^{3+} in the starting material was 1% of substituted Cd^{2+} ions. The sample studied had an irregular shape with dimensions between 6 and 15 mm and with two surface planes intersecting along the c-axis. All measurements were carried out with a constant magnetic field along this crystal axis. The high-frequency magnetic field $\boldsymbol{B}(t)$ was generated by a backward-wave oscillator with an output power between 2.8 and 55 mW. A detailed description of the spectrometer is given in Ref. [11]. To record the spectra, a magnetic field modulation at 15 kHz with a maximum amplitude of 8×10^{-4} T was produced by Helmholtz coils. Using the Voigt geometry we were able to align the high-frequency field $\boldsymbol{B}(t)$ along or transverse to the constant field $\boldsymbol{B}$ and to separate resonance transitions with different selection rules by rotating the polarization plane of the submillimeter radiation.

The measured electron-nuclear spectra have very complicated shapes which strongly depend on the direction of the high-frequency magnetic field $\boldsymbol{B}(t)$. Due to their specific hyperfine structures and their different slopes in the field dependence, it was possible to distinguish the signals from the single ion and the dimer center. For the

single ion in collinear constant and alternating magnetic fields, two resonance lines are observed with a well-resolved hyperfine structure consisting of eight lines [4]. One of these lines corresponds to a transition between the lower Zeeman sublevel of the ground doublet and the upper sublevel of the excited doublet. The second line, which shows a non-linear dependence of the resonance frequency on the magnetic field and disappears for $B>$ 5.5 T, provides evidence for strong mixing between the two other sublevels of these doublets. The corresponding signals assigned to doublet–doublet transitions in the dimer center are noticeably stronger. Some examples of the EPR spectra for the dimer centers are shown in Fig. 1. Superposition of the single ion hyperfine structure (the narrow lines on the high-field side of the recorded signal) and of the pair spectra at a frequency of 317 GHz can be seen in Fig. 1a. Doublet–doublet transitions without a change in sign of the electronic magnetic moment are observed for $\boldsymbol{B}(t)\perp\boldsymbol{B}$. In this case the allowed magnetic dipole transitions between the lower sublevel of the ground doublet and the nearest singlet Γ_2 are also observed. We assign these signals to the dimer center because the measured zero field splitting of 165 GHz coincides with the singlet energy obtained from optical data [8].

The shape of the EPR signals for the dimer centers (see Fig. 1) may be considered as a superposition of several electronic transitions having eight-component hyperfine structures of different intensity, shifted from each other by the inter-ion interaction. The field dependence of the individual resonance lines was observed down to zero field strength; all hyperfine splittings at zero field were measured.

There are some additional weak lines in the spectra recorded in collinear fields at frequencies close to the zero field splitting of the dimer center (see, for example, the low field side of the signal at 317 GHz in Fig. 1a). The origin of these lines is still unclear, they may correspond to transitions between excited states of the pair center.

3. Simulations of the spectra

We can consider the magnetic dipole–dipole interaction as the only interaction between two Ln^{3+} ions at a distance $R\approx 6$ Å from each other. The Hamiltonian of the dimer center has the form

$$H = H_1 + H_2 + \frac{(g_J\mu_B)^2}{R^3}(J_{x1}J_{x2} + J_{y1}J_{y2} - 2J_{z1}J_{z2}) \qquad (3)$$

where H_1 and H_2 are defined in Eq. (2). The crystal field states are strongly mixed by the Zeeman interaction. The spectral effects due to the hyperfine interaction and the dipole–dipole interaction are of comparable magnitude. Thus, a perturbative approach based on an effective spin Hamiltonian cannot give correct results in this case. We computed the spectra of the longitudinal and transverse electron-nuclear excitations (with the magnetic moments parallel and perpendicular to the magnetic field $\boldsymbol{B}$, respectively) for the dimer center by three successive simulations. In the first stage, the single ion Hamiltonian including the crystal field and the electronic Zeeman energies is diagonalized (matrix of 17 rank). In the next stage, we select the lowest five crystal field states ($\Gamma_3+\Gamma_2+\Gamma_3$) and compute the energy levels and wave functions of two equivalent ions coupled by the dipole–dipole interaction (matrix of 25 rank). In the last stage, neglecting simultaneous excitations of two single ion crystal field states, we select the 16 lowest electronic states of the pair of D_{3d} symmetry (four states, one doublet and two singlets, from the ground doublets, four states from the singlet Γ_2 and the ground doublet, and eight states from the first excited and the ground doublets) and introduce the hyperfine interactions. The spectrum of the mixed electron-nuclear states is obtained by diagonalizing the resulting matrix of 1024 rank. The envelopes of the absorption spectra were computed assuming a Gaussian line shape for the individual excitations with the same width of 0.5 GHz for all transi-

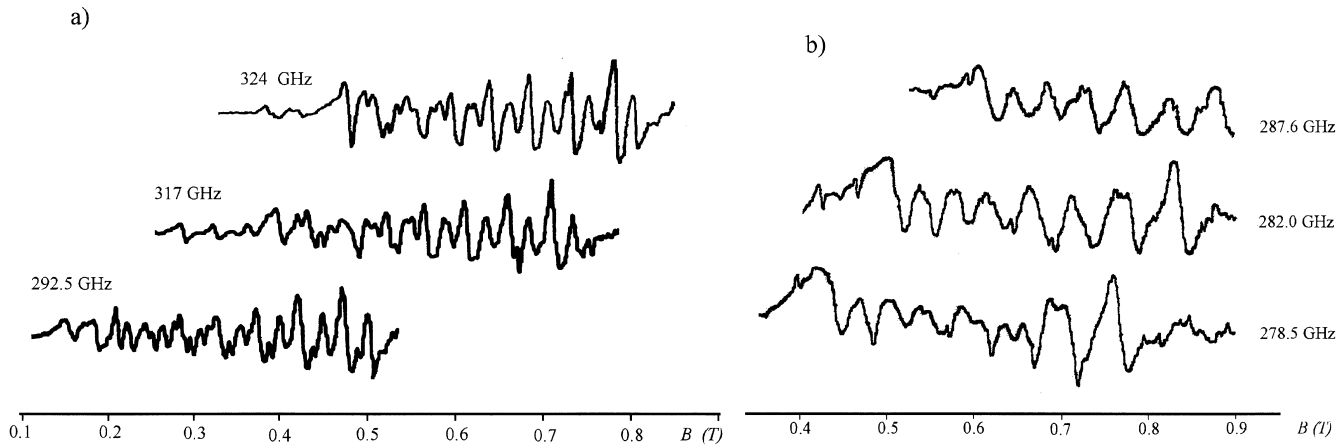

Fig. 1. Examples of the EPR signals from the Ho^{3+} symmetrical dimeric centers at different frequencies. Measurements were carried out in magnetic field $\boldsymbol{B}$ parallel to the symmetry c-axis of a lattice, and with high-frequency field $\boldsymbol{B}(t)\|\boldsymbol{B}$ (a) and $\boldsymbol{B}(t)\perp\boldsymbol{B}$ (b).

tions from the equally populated 256 electron-nuclear states derived from the single ion ground doublets. The square modules of the matrix elements of the operators $J_{z1} + J_{z2}$ and $J_{x1} + J_{x2}$, determining, respectively, the relative integral intensities of the longitudinal and transversal excitations, were calculated in the full basis of the 1024 electron-nuclear states. For several values of the magnetic field strength, the simulated absorption spectra obtained with the final set of the crystal field parameters ($B_2^0 = -75.6$, $B_4^0 = -94.3$, $B_6^0 = 12.75$, $B_4^3 = 2841$, $B_6^3 = 216.2$, $B_6^6 = 149.8\,\mathrm{cm}^{-1}$) are shown in Fig. 2. The calculated shifts of the peaks in the absorption spectra as a function of the magnetic field were compared with the experimental field dependence of the resonance frequencies and were used in a fitting procedure, which gave about the same values for the crystal field parameters as shown above. An example of the calculated field dependence of the frequencies of the longitudinal electron-nuclear excitations is presented in Fig. 3. Excitations belonging to the lower branch of the spectrum in Fig. 3 were not observed, perhaps due to strong absorption (the transmitted power is detected in our spectrometer) or non-effective modulation of the resonance frequencies in this band.

From the analysis of the EPR signals assigned to the single ion center, we determined the following crystal field parameters: $B_2^0 = -73.6$, $B_4^0 = -91.3$, $B_6^0 = 10.74$, $B_4^3 = 2720$, $B_6^3 = 285.0$, $B_6^6 = 103.2\,\mathrm{cm}^{-1}$. They do not differ substantially from the corresponding parameters for the dimer center. However, the performed simulations have shown that we cannot really distinguish between the EPR spectrum of a single Ho^{3+} ion with non-local charge compensation and a spectrum of a pair center consisting of non-equivalent ions (of the type Ho^{3+}–Cd^{2+}–Cd^{2+} vacancy–Ho^{3+}) with only slightly different crystal field splittings.

For the dimeric center, the crystal field splitting of the lower multiplets ^5I_J, $^5F_5$ was calculated with the reduced matrix elements of the Stevens operators from Ref. [12], and the final set of crystal field parameters given above. The calculated splittings of these multiplets are compared with the optical data in Table 1.

In conclusion, we would like to mention that when analyzing trends in the variation of the crystal field parameters for different lanthanide ions in $CsCdBr_3$ [13,14], one should remember that the values obtained in this work are model-dependent. Neglected contributions to

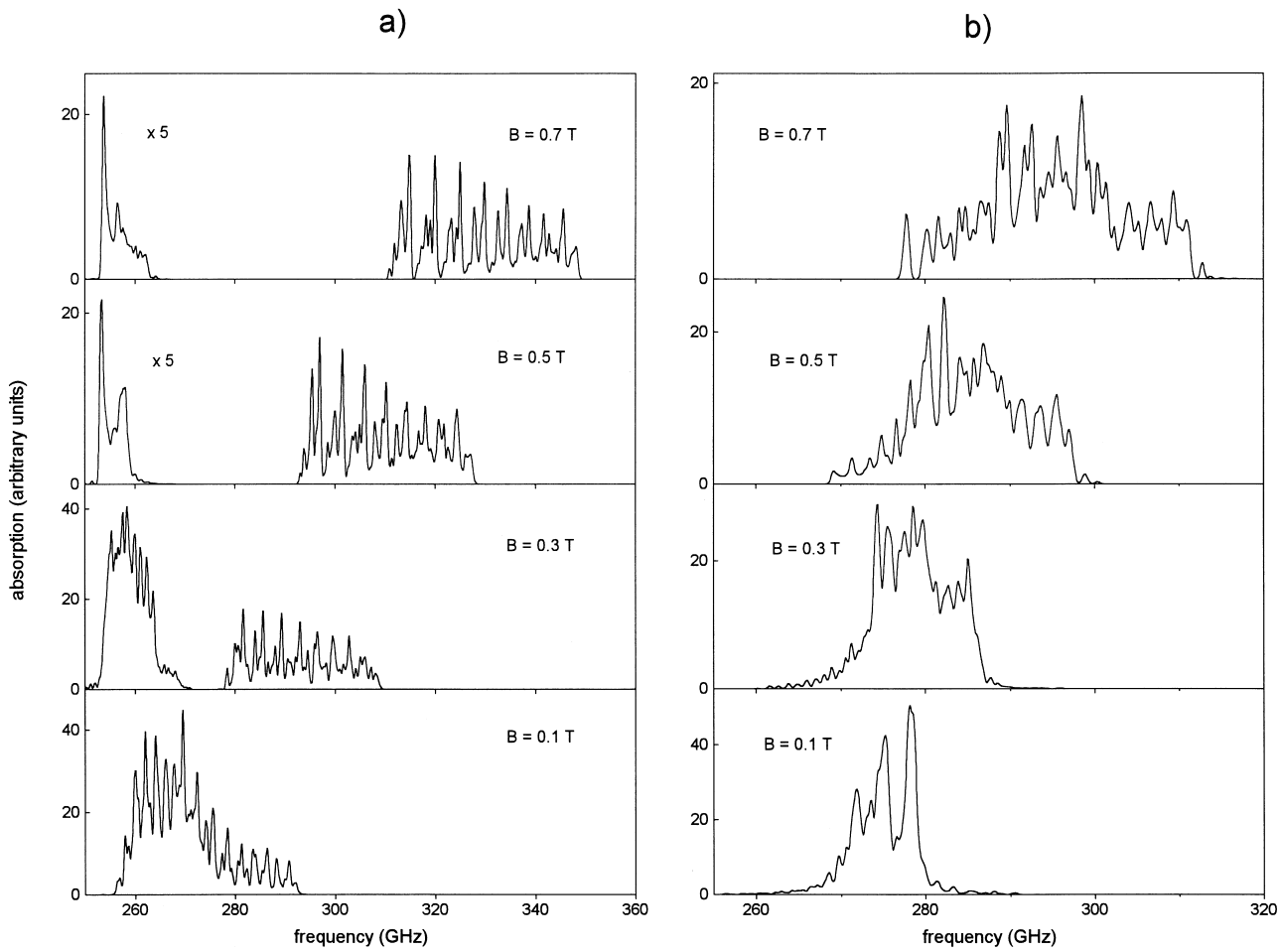

Fig. 2. Simulated absorption spectra of the pair symmetrical holmium center in the region of doublet–doublet transitions; (a) $\boldsymbol{B}(t)\|\boldsymbol{B}\|c$, (b) $\boldsymbol{B}(t)\perp\boldsymbol{B}\|c$.

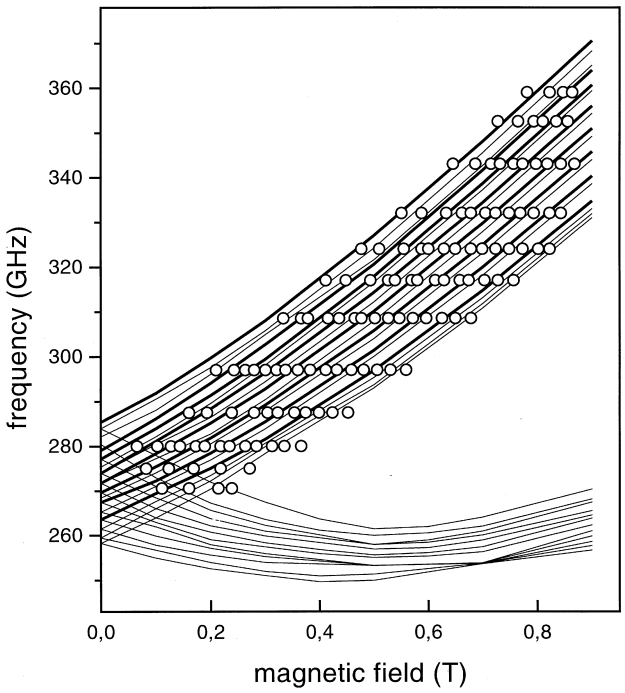

Fig. 3. Resonance frequencies of the longitudinal electron-nuclear excitations of the pair centers in $CsCdBr_3:Ho^{3+}$. Full curves represent results of calculations (the frequencies of the most intensive peaks in the absorption spectra were selected); data from EPR measurements are presented by circles.

the zero field splitting from the electron–phonon interaction, the two-electron correlated crystal field, and a renormalization of the magnetic moment of the 4f electrons due to the weak covalent bonding may substantially affect the parameters of the effective one-electron crystal field Hamiltonian.

Acknowledgements

This work was supported by RFBR grant N 96-02-18263. One of the authors (BZM) is grateful to the DAAD for funding a research visit to the Technical University of Darmstadt.

References

[1] J. Magarino, J. Tuchendler, P. Beauvillain, I. Laursen, Phys. Rev. B 21 (1980) 18.
[2] B.Z. Malkin, V.F. Tarasov, G.S. Shakurov, JETP Lett. 62 (1995) 811.
[3] H.P. Moll, J. van Tol, P. Wyder, M.S. Tagirov, D.A. Tayurskii, Phys. Rev. Lett. 77 (1996) 3459.
[4] V.F. Tarasov, G.S. Shakurov, B.Z. Malkin, A.I. Iskhakova, J. Heber, M. Altwein, JETP Lett. 65 (1997) 535.
[5] L.M. Henling, G.L. McPherson, Phys. Rev. B 16 (1977) 4756.
[6] J. Heber, M. Lange, M. Altwein, B.Z. Malkin, M.P. Rodionova, J. Alloys Comp., (this issue).
[7] P.A. Tanner, V.V. Ravi Kanth Kumar, C.K. Jayasankar, M.F. Reid, J. Alloys Comp. 215 (1994) 349.
[8] M. Mujaji, G.D. Jones, R.W.G. Syme, Phys. Rev. B 48 (1993) 710.
[9] M.A.H. McCausland, I.S. Mackenzie, Adv. Phys. 28 (1979) 305.
[10] J. Neukum, N. Bodenschatz, J. Heber, Phys. Rev. B 50 (1994) 3536.
[11] V.F. Tarasov, G.S. Shakurov, Appl. Magn. Res. 2 (1991) 571.
[12] K. Rajnak, W. Krupke, J. Chem. Phys. 46 (1967) 3532.
[13] F. Pelle, N. Gardant, M. Genotelle, Ph. Goldner, P. Porcher, J. Phys. Chem. Solids 56 (1995) 1003.
[14] E. Antic-Fidancev, M. Lemaitre-Blaise, J-P. Chaminade, P. Porcher, J. Alloys Comp. 225 (1995) 95.